American Mineralogist, Volume 75, pages 1253–1267, 1990

A study of the mean-square displacement amplitudes of Si, Al, and O atoms in framework structures: Evidence for rigid bonds, order, twinning, and stacking faults

R. T. Downs, G. V. Gibbs
Department of Geological Sciences, Virginia Polytechnic Institute and State University, Blacksburg, Virginia 24061, U.S.A.

M. B. Boisen, Jr.
Department of Mathematics, Virginia Polytechnic Institute and State University, Blacksburg, Virginia 24061, U.S.A.

Abstract

A study of the mean-square displacement amplitudes (MSDA) of the T(Al,Si) and O atoms in ordered framework silicates and aluminosilicates indicates that the sizes, shapes, and orientations of the displacement ellipsoids in these crystals are consistent with a rigid bond model. In particular, the MSDAs of the T and O atoms in the direction of the TO bonds tend to be equal and to increase with temperature. When this relationship does not hold, it appears to be related to the presence of static disorder. This observation leads to criteria that may be used to detect disorder in crystals. A simple rigid bond model is presented that, to a reasonable degree, describes the ellipticity and the orientation of the displacement ellipsoids of the bridging O atoms.

Introduction

An examination of the isotropic displacement factors of the O atoms, B(O), recorded for framework silicates shows that two distinct populations can be defined, one with values ranging between 0.25 and 3.0 Å^2 with a concentration near 1.0 and the other with values spread rather uniformly between 4.5 and 10.0 Å^2 (Boisen et al., 1990). A stepwise regression analysis of the apparent SiO bond length data, R(SiO), for the silica polymorphs making up the first population indicates that R(SiO) correlates with such parameters as fs(O), fs(Si) (the fraction of s character of the orbitals on O and Si, respectively, involved in bond formation), B(O), and P, the pressure at which the diffraction data were recorded. A similar regression analysis of the bond-length data for the second population indicates that R(SiO) correlates only with B(O), the other parameters failing to make a significant contribution to the regression sum of squares (see also Liebau, 1985). The tridymite and clathrasil crystals that constitute the bulk of this population are typically twinned (Kato and Nukui, 1976; Kihara, 1978; Gies, 1983, 1984, 1986), a feature that has been ascribed in tridymite to the presence of stacking faults and disorder in layers of silicate tetrahedra (Flörke, 1954, 1955).

In this paper, the mean-square displacement amplitudes (MSDA) of the Si and O atoms are calculated in the direction of the SiO bonds for the silica polymorphs coesite, quartz, and low cristobalite, using the anisotropic Gaussian displacement parameters (ADP), reported in structural refinements. Similar calculations are presented for clathrasil and tridymite crystals and a variety of aluminosilicate framework structures. It is noteworthy that Zachariasen observed in 1969 that the ADPs recorded prior to that time "are all nonsense and must all be done again in a sensible way." However, our study indicates that those recorded for ordered framework silicates and aluminosilicates since about 1975 do indeed make sense and may be used to improve our understanding of the vibrational modes of the atoms and to provide a measure of the perfection of a crystal. It also suggests that the TO bonds (T = Al,Si) in the silica polymorphs and ordered aluminosilicate framework structures behave as rigid units with the T and O atoms appearing to vibrate along the bonds in tandem. Criteria based on MSDA data are presented for testing whether a structure possesses substitutional and positional disorder such as twinning and stacking faults. An examination of how a rigid bond model relates to the orientations and the shapes of the displacement ellipsoids of the O atoms in ordered silicate and aluminosilicate framework structures (Downs, 1989) appears in Appendix 1.

Mean-square displacement amplitudes and evidence for dynamic and static disorder

If the AB bonds between atoms A and B composing an AB$_n$-coordinated polyhedron in a crystal are rigid, then one would expect that the atoms should appear to vibrate in tandem along each AB bond, and so the MSDA of A toward B, z^2_{AB}, and that of B toward A, z^2_{BA}, should tend to be equal (Hirshfeld, 1976; Dunitz et al., 1988). If the

0003–004X/90/1112–1253$02.00

displacement parameters of these atoms define anisotropic ellipsoids and if the bonds are measured at a variety of temperatures, then a linear correlation between z^2_{AB} and z^2_{BA} should be observed. The extent to which the correlation is developed should depend on the extent to which the MSDAs depend on the static (substitutional and positional disorder, twinning and stacking faults) and the dynamic (thermal and zero-point motion) disorder exhibited by the atoms. The MSDAs should also depend on the charge-density deformation ascribed to the formation of chemical bonds (Hirshfeld, 1976). This effect will be ignored since, for example, the equivalent isotropic displacement factors recorded in a monopole refinement of the charge density for coesite are only about 5% larger than those recorded in a refinement with higher multipoles (Geisinger et al., 1987).

Mean-square displacement amplitudes for Si and O along SiO bonds of framework silicates

In this paper, we only include the data used by Boisen et al. (1990) for which anisotropic refinements have been completed at room pressure. Thus, our first population, denoted population I, consists of 96 R(SiO) bond-length data recorded for the coesite structure (Gibbs et al., 1977b; Levien and Prewitt, 1981; Kirfel and Will, 1984; Smyth et al., 1987; Geisinger et al., 1987), the low cristobalite structure (Peacor, 1973), the low quartz structure (Young and Post, 1962; LePage and Donnay, 1976; Levien et al., 1980; Wright and Lehmann, 1981), and the high quartz structure (Wright and Lehmann, 1981) that have B(O) values less than 3.0 Å^2. Our second population, denoted population II, consists of 181 R(SiO) data recorded in several studies of clathrate structures (Gies, 1983, 1984, 1986; Gerke and Gies, 1984) and tridymite crystal structures (Dollase, 1967; Kihara, 1977, 1978; Kihara et al., 1986a, 1986b) that have B(O) values greater than 4.0 Å^2.

Our software, Metric, was used to calculate z^2_{SiO} and z^2_{OSi} from the ADPs recorded for each Si and O atom forming the SiO bonds of the two populations. Figure 1 is a scatter diagram of z^2_{SiO} vs. z^2_{OSi} calculated for the SiO bonds of population I. The slope of the regression line for this data is 0.99, the intercept is −0.00006 Å^2, and the coefficient of determination is $r^2 = 0.98$. As the estimated slope and intercept are not significantly different from 1.0 and 0.0, respectively, we conclude that the MSDAs measured for the Si and O atoms of quartz, coesite, and cristobalite conform with a trend expected for a set of SiO bonds behaving as rigid units. We also conclude that the ADPs recorded for these minerals appear to provide a reasonable measure of the dynamic disorder of the Si and O atoms in these crystals. A calculation of $\Delta = z^2_{OSi} - z^2_{SiO}$ for these minerals shows a maximum deviation from zero of ±0.0015 Å^2, which conforms with that (±0.001 Å^2) proposed for the rigid covalent CC bonds in several molecular crystals (Hirshfeld, 1976) and with that (±0.0007 Å^2) measured for the SiO bonds in the single chains of silicate tetrahedra in enstatite (Ghose et al., 1986), but which is somewhat smaller than that (±0.003 Å^2) recorded for the more ionic bonds in a variety of transition-metal complexes (Bürgi, 1984).

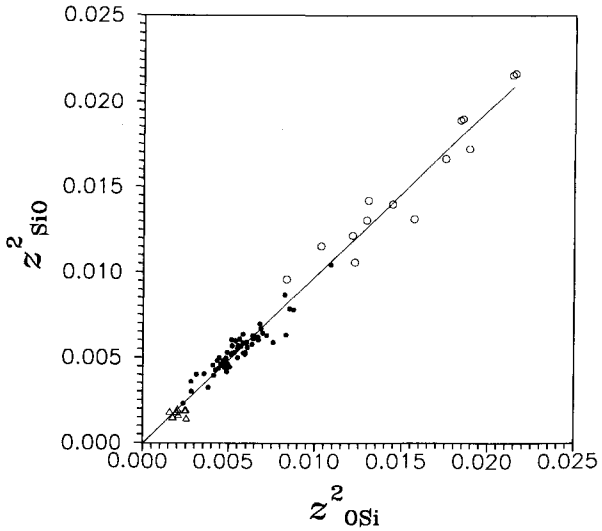

Fig. 1. A scatter diagram of the mean-square displacement amplitudes, z^2_{SiO} vs. z^2_{OSi} calculated in the direction of the SiO bonds for Si and O, respectively, for the framework silicates coesite, quartz, and cristobalite (population I). The MSDAs recorded at low temperatures (15 K) are plotted as open triangles, those recorded at room temperature are plotted as closed circles, and those reported at elevated temperatures up to 860 K are plotted as open circles. The regression equation is $z^2_{SiO} = -0.00006 + 0.992 z^2_{OSi}$ where $\sigma(-0.00006) = 0.00012$ Å^2, $\sigma(0.992) = 0.015$, and the coefficient of determination is $r^2 = 0.98$.

A scatter diagram of z^2_{SiO} vs. z^2_{OSi} prepared for the O and Si atoms forming the bonds of population II shows a

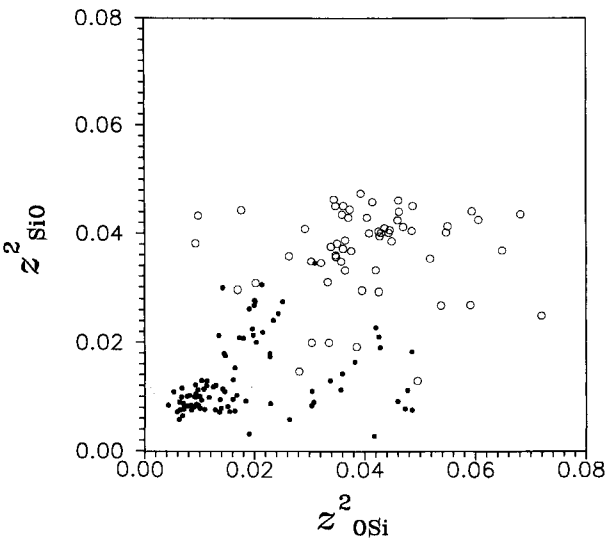

Fig. 2. The MSDAs, z^2_{SiO} vs. z^2_{OSi} for the SiO bonds in the clathrates and tridymite structures (population II). The data recorded at room temperature are plotted as solid circles and those recorded at higher temperatures are plotted as open circles.

relatively wide scatter of points (see Fig. 2). This suggests that the ADPs measured for these minerals describe a significant component of static disorder. Considering the relatively wide scatter of these points, it appears that a significant fraction of the atoms in the clathrates and the tridymite structures of population II are probably displaced from the positions that they would occupy in domains that are free of twinning and other structural defects. A refinement of a set of diffraction data recorded for such crystals would be expected to yield a set of specious positional parameters and ADPs. With increasing disorder, the B values of the atoms in these crystals are expected to increase in magnitude, and the apparent bond lengths calculated from these positional parameters are expected to shorten. This implies that R(SiO) should correlate inversely with both B(O) and B(Si) for population II. The linear regression analyses of these data shows that B(O) and B(Si) are each highly correlated with R(SiO) (Boisen et al., 1990). However, in a stepwise regression analysis involving B(O), B(Si), fs(O), and fs(Si), only B(O) makes a significant contribution to the regression sum of squares, correlating inversely with R(SiO).

Mean-square displacements of T and O atoms along TO bonds of ordered and disordered alkali feldspars

The structure of feldspar consists of a framework of corner-sharing TO_4 tetrahedra with either monovalent or divalent cations tucked into the available cavities to neutralize the overall charge of the framework. As is well known, the alkali feldspars are believed to exhibit a variety of structural states ranging from a disordered state, in which the Al and Si atoms are randomly distributed among all of the TO_4 groups, to a configuration in which these atoms are ordered into an array of translationally equivalent SiO_4 and AlO_4 groups. As argued by Smith (1954) and Smith and Bailey (1963), the mean TO bond length, $\langle R(\mathrm{TO})\rangle$, for a given TO_4 group in feldspar is believed to vary linearly with Al content from 1.61 Å for a TO_4 group containing only Si to 1.75 Å for a group containing only Al. As the alkali feldspars are believed to exhibit a continuum of intermediate structural states ranging between ordered and disordered configurations, we have an opportunity to examine how $\Delta = z^2_{\mathrm{OT}} - z^2_{\mathrm{TO}}$ varies with structural state. We also have an opportunity to examine how scatter diagrams of z^2_{TO} vs. z^2_{OT} for structures that exhibit substitutional disorder compare with those obtained for structures believed to exhibit disorder ascribed to stacking faults and twinning. In addition, we may see the effects that the nonframework Na^{+1} and K^{+1} cations have on the MSDAs.

Bürgi (1989) has published a scatter diagram prepared by Kunz and Armbruster (1990) for both ordered and disordered alkali feldspars of the average value of Δ, $\langle\Delta\rangle$, for 138 TO_4 tetrahedra vs. $\langle R(\mathrm{TO})\rangle$ and has found that $\langle\Delta\rangle$ varies as a quadratic function of $\langle R(\mathrm{TO})\rangle$ according to the theoretical equation

$$\langle\Delta_t\rangle = [1.744 - \langle R(\mathrm{TO})\rangle] \times [\langle R(\mathrm{TO})\rangle - 1.607]. \quad (1)$$

An examination of the Kunz-Armbruster diagram shows that $\langle\Delta\rangle$ is smallest (± 0.0015 Å^2) for the Al-rich and Si-rich tetrahedra in the ordered feldspars low albite and low microcline, whereas it is as large as ± 0.007 Å^2 for the disordered and partly ordered tetrahedra in intermediate albite and microcline, orthoclase, high albite, and sanidine. The $\langle\Delta\rangle$ values obtained for the Si-rich and Al-rich tetrahedra are in close agreement with those observed for the silicate tetrahedra of the framework silicates used to prepare Figure 1 (see Table 1).

As both low albite and low microcline are believed to contain an ordered array of Al-rich and Si-rich tetrahedra, we plotted z^2_{TO} vs. z^2_{OT} for the 160 TO bonds for these feldspars in Figure 3 to learn how such a plot compares with that prepared for quartz, coesite, and cristobalite. The data were taken from Winter et al. (1977), Harlow and Brown (1980), Strob (1981), Blasi et al. (1984), Smith et al. (1986), Blasi et al. (1987), and Armbruster et al. (1990). As these data were collected over a wide range of temperatures from 13 K to 1263 K, the range of the MSDA values recorded for this data set is significantly larger than that recorded for the silica polymorphs whose data sets were measured over a smaller temperature range, between 15 K and 860 K.

A linear regression analysis of the data used to prepare Figure 3 yields a slope of 0.94, an intercept of -0.00008 Å^2, and a coefficient of determination of $r^2 = 0.99$. As the slope of the regression line departs from the ideal 45° line by only 1.8°, we conclude that these data are consistent, for the most part, with the Megaw (1974) view of the feldspar structure as an engineering construct of rigid rods connected together with TOT angle brackets "made of springy material." This is further supported by a study (Bartelmehs et al., in preparation) of the rigid-body motion of the TO_4 groups in the ordered silica polymorphs and feldspars that shows that the MSDAs associated with the O atoms in the directions of the intratetrahedral O atoms are linearly correlated, whereas those between intertetrahedral O atoms are substantially less so.

Because the $\langle\Delta\rangle$ values measured for low albite and microcline match those measured for quartz, coesite, and cristobalite, we conclude that the component of substitutional disorder in these feldspars is probably small, if not absent. Although the intercept of the line calculated for these feldspars is not significantly different from 0.0, the slope of the line is significantly less than the ideal value of 1.0. This indicates, as discussed later, that z^2_{OT} tends to increase with temperature at a somewhat faster rate than z^2_{TO}, unlike the silica polymorphs, where both of these parameters appear to increase at about the same rate. As the feldspars, unlike the silica polymorphs, contain nontetrahedral cations, the departure of the slope from the ideal value may depend in part on the bonds formed between these cations and the O atoms of the framework.

The Al and Si atoms in the alkali feldspars, high albite

TABLE 1. Silica polymorphs and aluminosilicate frameworks that satisfy the rigid-bond criteria of this paper

Mineral	Reference	⟨⟨Δ⟩⟩	Esd
Quartz	Young and Post (1962)	−0.00073	0.00018
Quartz	Zachariasen and Plettinger (1965), type II	0.00187	0.00018
Quartz	LePage and Donnay (1976)	0.00053	0.00001
Quartz	Levien et al. (1980)	0.00082	0.00017
Quartz	Wright and Lehmann (1981), at 25 °C	−0.00016	0.00040
High quartz	Wright and Lehmann (1981), natural at 590 °C	−0.00037	—
High quartz	Wright and Lehmann (1981), synthetic at 590 °C	−0.00065	—
Cristobalite	Peacor (1973), at 28 °C	0.00001	0.00051
Cristobalite	Peacor (1973), at 65 °C	−0.00123	0.00001
Cristobalite	Peacor (1973), at 103 °C	0.00076	0.00105
Cristobalite	Peacor (1973), at 142 °C	−0.00062	0.00066
Cristobalite	Peacor (1973), at 179 °C	0.00170	0.00096
Cristobalite	Peacor (1973), at 210 °C	0.00105	0.00073
Coesite	Gibbs et al. (1977b)	−0.00006	0.00054
Coesite	Levien and Prewitt (1981)	0.00049	0.00030
Coesite	Kirfel and Will (1984)	0.00004	0.00020
Coesite	Smyth et al. (1987), at 15 K	0.00036	0.00041
Coesite	Smyth et al. (1987), at 292 K	0.00052	0.00017
Coesite	Geisinger et al. (1987), IAM refinement	0.00003	0.00010
Coesite	Geisinger et al. (1987), IAM + refinement	−0.00042	0.00024
Low albite	Winter et al. (1977), at 500 °C	0.00130	0.00061
Low albite	Winter et al. (1977), at 750 °C	0.00135	0.00062
Low albite	Winter et al. (1977), at 970 °C	0.00156	0.00098
Low albite	Harlow and Brown (1980), neutron	0.00035	0.00035
Low albite	Harlow and Brown (1980), X-ray	0.00177	0.00090
Low albite	Smith et al. (1986), at 13 K	0.00035	0.00018
Low albite	Armbruster et al. (1990)	0.00028	0.00033
Microcline	Strob (1981)	−0.00005	0.00027
Microcline	Blasi et al. (1984), sample 7813A	0.00115	0.00120
Microcline	Blasi et al. (1984), sample 7813B	0.00060	0.00116
Microcline	Blasi et al. (1987)	0.00085	0.00078
Slawsonite	Griffen et al. (1977)	0.00125	0.00096
Low cordierite	Cohen et al. (1977), X-ray	0.00107	0.00086
Low cordierite	Cohen et al. (1977), neutron	0.00060	0.00100
Low cordierite	Hochella et al. (1979), at 375 °C, White Well	0.00009	0.00133
Low cordierite	Wallace and Wenk (1980), sample Sci 624	0.00117	0.00074
Low cordierite	Wallace and Wenk (1980), sample Sci 1018	0.00188	0.00046
Low cordierite	Armbruster (1986a), from Ferry	0.00047	0.00067
Low cordierite	Armbruster (1986a), from Haddam	0.00060	0.00056
Low cordierite	Armbruster (1986a), from Sponda	0.00050	0.00055
Low cordierite	Armbruster (1986a), from Kemiö	0.00077	0.00121
Low cordierite	Armbruster (1986b), at 100 K	0.00063	0.00066
Low cordierite	Armbruster (1986b), at 500 K	0.00027	0.00065
Bikitaite	Bissert and Liebau (1986)	0.00061	0.00082
Edingtonite	Galli (1976), *C*2,2,2	0.00119	0.00121
Edingtonite	Kvick and Smith (1983), *C*2,2,2	0.00063	0.00058
Mesolite	Artioli et al. (1986b)	0.00056	0.00060
Natrolite	Artioli et al. (1984)	0.00038	0.00029
Scolecite	Kvick et al. (1985)	0.00040	0.00026
Thomsonite	Pluth et al. (1985b)	0.00057	0.00047
Yugawaralite	Kvick et al. (1986)	0.00084	0.00059

and sanidine, are believed to be disordered over the TO_4 tetrahedra of their structures. A plot of z^2_{TO} vs. z^2_{OT} for their TO bonds was prepared (Fig. 4) to learn how it compares with the one for the clathrasils and the tridymites, on the one hand, and with the one for low albite and low microcline, on the other. The 162 data points used to prepare the figure were taken from refinements by Weitz (1972), Phillips and Ribbe (1973), Keefer and Brown (1978), Winter et al. (1979), Blasi et al. (1981), and Scambos et al. (1987). The data scatter in a moderately wide band along the regression line drawn in Figure 4, with an r^2 value of 0.92. The cluster of points at the bottom right of the figure that seems to depart from the trend of the remaining data is for an Eifel sanidine refined at room temperature by Weitz (1972) (see discussion below).

A comparison of Figures 1–4 reveals several distinguishing features: (1) the data for the silica polymorphs (Fig. 1) and the ordered feldspars (Fig. 3) are statistically identical with the predictions of the rigid bond model for a set of ordered crystals largely free from defects; (2) the data for the clathrasils and tridymite scatter rather widely over much of the field of Figure 2, suggesting that these crystals contain a significant number of defects that may be ascribed to twinning and stacking faults; and (3) the data for high albite and sanidine (Fig. 4) are spread rather uniformly along a moderately wide band that parallels the line recorded for low albite and low microcline (Fig. 3), but the intercept (−0.0037 Å^2) of the line fit to the data, without the Eifel data, is significantly smaller than 0.0, the intercept obtained for both the framework silicates and for low albite and low microcline.

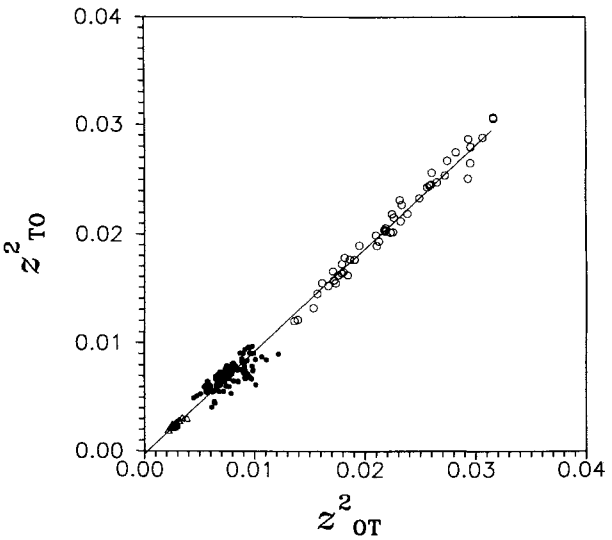

Fig. 3. The MSDAs, z^2_{TO} vs. z^2_{OT} for the T and O atoms recorded for low albite and low microcline. The data recorded at low temperatures (13 K) are plotted as open triangles, those recorded at room temperature are plotted as closed circles, and those recorded at elevated temperatures up to 1263 K are plotted as open circles. The regression equation is $z^2_{SiO} = -0.00008 + 0.940z^2_{OSi}$ where $\sigma(-0.00008) = 0.00011$ Å^2, $\sigma(0.940) = 0.008$, and the coefficient of determination is $r^2 = 0.99$.

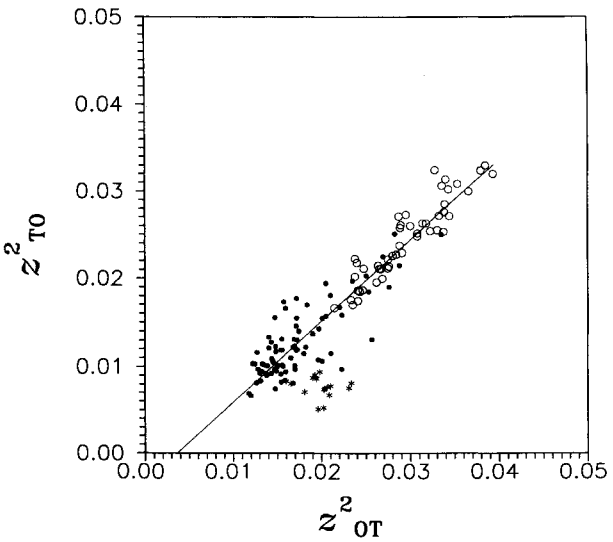

Fig. 4. A scatter diagram of z^2_{TO} vs. z^2_{OT} for high albite and sanidine. The room temperature data are plotted as closed circles, the data recorded at high temperatures are plotted as open circles, and the Eifel data are plotted as stars. The regression equation without the Eifel data is $z^2_{TO} = -0.0037 + 0.945z^2_{OT}$ where $\sigma(-0.0037) = 0.0006$ Å^2, $\sigma(0.945) = 0.023$, and the coefficient of determination is $r^2 = 0.92$.

The larger scatter of data and the departure of the intercept from 0.0 for high albite and sanidine may be ascribed to substitutional disorder. If we assume that there is complete substitutional disorder in high albite and sanidine, then each TO_4 group would contain 25% Al, on average. With Bürgi's (1989) assumption that R(SiO) = 1.607 Å and R(AlO) = 1.744 Å for ordered feldspar structures (see Eq. 1), the Smith and Bailey (1963) assumption that $\langle R(TO)\rangle$ varies linearly with the fraction, f, of Al in a TO_4 group and that $\Delta R = R(AlO) - R(SiO) = 1.744 - 1.607 = 0.137$ Å, then Equation 1 becomes

$$\langle \Delta_t \rangle = (1 - f)f(\Delta R)^2 = (1 - f)f(0.137)^2. \quad (2)$$

Hence, with $f = 0.25$, $\langle \Delta_t \rangle = \langle z^2_{OT} - z^2_{TO} \rangle = 0.0035$ Å^2. This implies that $\langle z^2_{TO} \rangle = -0.0035 + \langle z^2_{OT} \rangle$, predicting an intercept of -0.0035 Å^2 close to the observed value. As the slope found for the regression equation for high albite and sanidine is significantly different from 1.0, it appears that the experimental line is statistically different from that predicted by Bürgi's equation. However, the slope of the line departs by only 1.6° from the ideal value. This small departure suggests that the experimental data conform, to a first approximation, with the theoretical trend predicted by the equation.

The departure of the intercept of the regression line observed for high albite and sanidine from 0.0 may also be rationalized with Bürgi's equation. In the derivation of his equation, Bürgi (1989) assumed that each T atom is fixed in space regardless of whether T is Al or Si, whereas the coordinating O atoms are located, on average, a distance of 1.744 Å away when T is Al, or 1.607 Å when it is Si. It is argued that the substitutional disorder causes the displacement ellipsoids of the O atoms to be elongated in the direction of the TO bonds. When the disorder is complete for $f = 0.25$, then the amount of elongation should be fairly constant with the value of z^2_{OT} being 0.0035 Å^2 larger than that of z^2_{TO} along the same bond. When $f = 0.5$, the maximum allowable value in a feldspar, Equation 2 yields a maximum expected $\langle \Delta_t \rangle$ value of 0.0047 Å^2. When the $\langle \Delta \rangle$ values of a structure exceed this value, types of disorder other than substitutional should be considered.

The departure of the slopes for both the ordered and disordered feldspars from the ideal 45° line may be related to an increase in the optical mode vibrations of the T and O atoms accompanying an increase in temperature at high temperatures (Megaw, 1973) as well as to the bonding requirements of the nontetrahedral cations. The feldspar data with the larger MSDAs in Figures 3 and 4, which influence the slope, were recorded at temperatures as high as 1273 K. We would expect, at this high temperature, that the vibrational amplitude of the lighter O atom would increase at a slightly faster rate than that of the heavier T atom with increasing temperature. This would result in z^2_{OT} increasing at a faster rate than z^2_{TO}, providing an explanation, at least in part, for the small but significant departure of the slope from 45°.

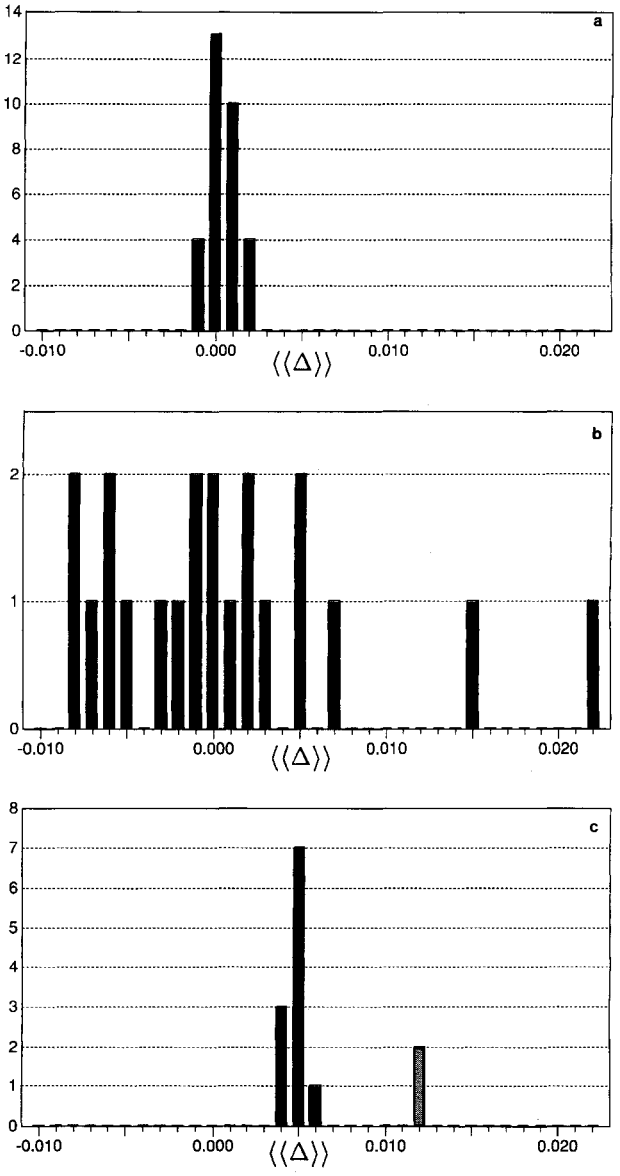

Fig. 5. (a) Histograms of $\langle\langle\Delta\rangle\rangle$ (Å^2) for the ordered structures of low albite, low microcline, quartz, cristobalite, and coesite; (b) for the disordered structures of tridymite and the clathrasils; and (c) for the substitutionally disordered high albite and sanidine. The Eifel sanidine is marked with stipples.

Criteria for recognizing ordered structures with rigid TO bonds, structures with substitutional disorder, and those with twinning and stacking faults

The structures of the silica polymorphs and the aluminosilicates appear to be composed of rigid TO bonds, as demonstrated by the equality of z^2_{TO} and z^2_{OT} for low albite, low microcline, quartz, cristobalite, and coesite. This implies that the vibrational modes of these atoms in these crystals are largely acoustical in nature, with the T and O atoms being displaced in phase along the TO bonds as rigid units (Willis and Pryor, 1975). This also implies that $\langle\Delta\rangle$ should be close to zero, on average, for such tetrahedra in these structures.

If we define $\langle\langle\Delta\rangle\rangle$ to be the average of all $\langle\Delta\rangle$ values in a structure, then $\langle\langle\Delta\rangle\rangle$ should also be close to zero. Furthermore, the estimated standard deviation, esd, of $\langle\langle\Delta\rangle\rangle$ should also be small, since the range of the $\langle\Delta\rangle$ values is small. A histogram of $\langle\langle\Delta\rangle\rangle$ prepared for low albite, low microcline, quartz, cristobalite, and coesite (Fig. 5a) shows that the $\langle\langle\Delta\rangle\rangle$ values for these structures range between -0.00123 and 0.00187 Å^2. The frequency distribution of estimated standard deviations of the $\langle\langle\Delta\rangle\rangle$ values that we calculate for these structures is plotted in Figure 6a, which shows a maximum esd of 0.00120 Å^2. Histograms of $\langle\langle\Delta\rangle\rangle$ and its esd prepared for the clathrasils and tridymites (Figs. 5b and 6b, respectively) show a much larger range of $\langle\langle\Delta\rangle\rangle$ values than recorded for the ordered feldspars and the framework silicates coesite, quartz, and low cristobalite, from -0.00777 to 0.02166 Å^2, with esd as large as 0.01996 Å^2.

Histograms of $\langle\langle\Delta\rangle\rangle$ and its esd prepared for the disordered feldspars sanidine and high albite are presented in Figures 5c and 6c, respectively. All of these data, with the exception of the Eifel sanidine data, fall within the range of $\langle\langle\Delta\rangle\rangle$ values of 0.00388 to 0.00553 Å^2, the range expected for disordered feldspar with Al/Si ratios between 0.25 and 0.50. The $\langle\langle\Delta\rangle\rangle$ values for the Eifel sanidine (0.012 Å^2) fall outside this range. In fact, they are similar to those exhibited by the clathrasils and the tridymites. In view of the large $\langle\langle\Delta\rangle\rangle$ values recorded for this feldspar, the evidence suggests that it contains static disorder like that indicated for the clathrasils and the tridymites. This would provide a possible explanation, as touched on earlier, for why the Eifel data fall off the linear trend in Figure 4.

Based on the histograms for the ordered feldspars and the silica polymorphs (Figs. 5a and 6a), rigid bond criteria for TO bonds in framework structures are suggested that may be used to define the relative perfection of a crystal. If the TO bonds in an ordered structure behave as rigid units, then the following two criteria should be satisfied: (1) -0.00125 Å$^2 \leq \langle\langle\Delta\rangle\rangle \leq 0.002$ Å^2 and (2) the esd of $\langle\langle\Delta\rangle\rangle \leq 0.00125$ Å^2.

In an application of these criteria, we calculated the $\langle\langle\Delta\rangle\rangle$ values and their esd for 143 framework silicate and aluminosilicate structures. Those that satisfy the two criteria are listed in Table 1 and those that fail either one or both are listed in Table 2.

An examination of the data in these tables shows that although five of the refined quartz structures satisfy the rigid-bond criteria, five also do not. The quartz data published by Lager et al. (1982) were determined from a refinement of powder data rather than from single-crystal data. As a single-crystal data set is typically more precise and larger in size than a corresponding powder data set, the failure of the Lager refinements to satisfy both criteria

is not unexpected. The Smith and Alexander (1963) data set appears to have been refined with the wrong symmetry constraints imposed on the displacement parameters of the atoms (Zachariasen and Plettinger, 1965), thus possibly explaining the failure of the criteria for this quartz refinement. The quartz data presented by Zachariasen and Plettinger (1965) were obtained in refinements where two different extinction correction models were tested. The quartz structure refined with their type II model met the criteria whereas that refined with the type I did not, suggesting that the type II model may be the more appropriate extinction model. In all the cases examined for quartz, failure to satisfy the criteria seems to depend on refinement strategies and on how the data were recorded and seems to be independent of the crystals themselves. This is surprising because twinning is the rule rather than the exception in quartz (Frondel, 1962).

In a neutron diffraction study of the structure of quartz at temperatures up to 860 K, Wright and Lehmann (1981) conclude that the O atom in high quartz may be disordered into a split-atom general position related by the Dauphiné twin law. This result is contrary to results obtained in an earlier X-ray diffraction study, which suggests that the O atom is ordered at a special position (Young, unpublished data, 1962). A calculation of the MSDAs obtained from the refined ADPs (Wright and Lehmann, 1981) with the O atom in a special position shows that the structure satisfies the criteria set forth in this paper, suggesting that the O atom is ordered. A second refinement of the neutron diffraction data, assuming that the O atom is randomly distributed in a general position, resulted in a significant reduction in the R factor. Not only do the MSDAs obtained in this refinement fail to meet the criteria, but the resulting SiO bond lengths are also significantly different from one another (1.560, 1.640 Å) and from that (1.61 Å) recorded for low quartz and other silica polymorphs. Furthermore, the resulting displacement parameters of the O atom are significantly more anisotropic than those of the Si atom. If the disorder in high quartz is static and related by the Dauphiné twin law, then we would expect that the displacement parameters of the Si atom would also show a relatively large anisotropy because of the rigid nature of the SiO bonds. A model for high quartz based on the librations of rigid silicate tetrahedra may provide an explanation for the highly anisotropic nature of the O atom and the less anisotropic nature of Si, without resorting to the use of a split O atom model. Such a model seems reasonable in view of the observation that the average libration angle calculated for the silicate tetrahedron based on their refinement of high quartz with O in the special position yields a value that is slightly smaller (8.4°) than that obtained in an extrapolation (9.0°) of such data recorded in a high temperature study of low cristobalite (Peacor, 1973). Given this result, the discrepancy in the observed SiO bond lengths and the observation that the MSDAs obtained in the split atom refinement fail to meet the criteria support Young's (unpublished data, 1962) conclusion that the O atom in high quartz is ordered at a special position. A modeling of the molecular dynamics of the quartz structure as a function of temperature by Tsuneyuki et al. (1990) also supports this conclusion by predicting that low-quartz transforms to high quartz, with the O atom in the special position, at some temperature above 850 K.

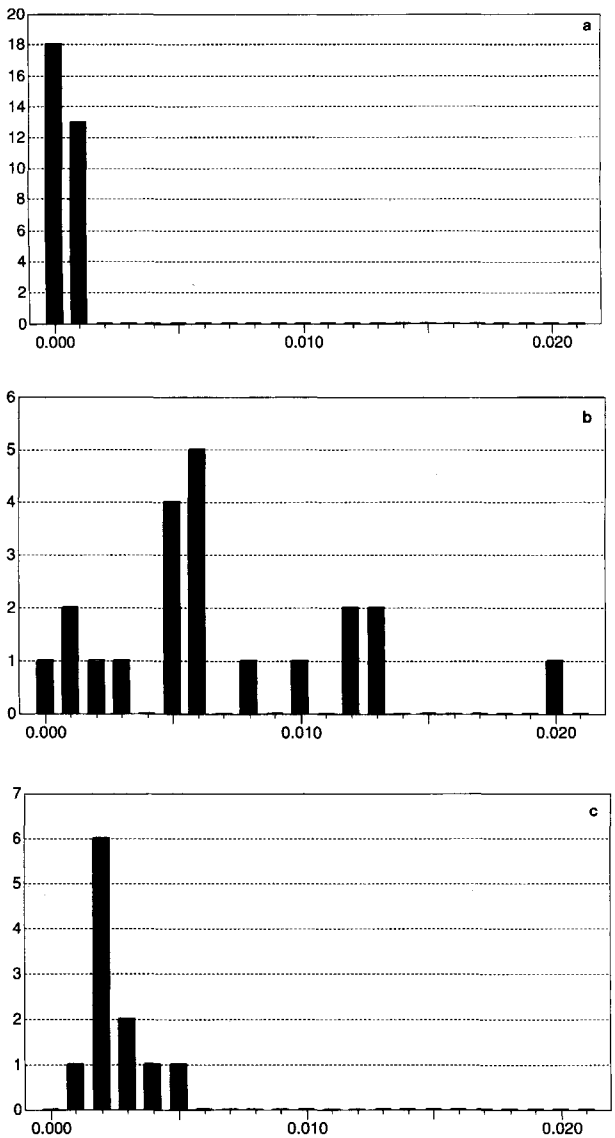

Fig. 6. (a) Histograms of the esd of $\langle\langle\Delta\rangle\rangle$ (Å^2) for the ordered structures: low albite, low microcline, quartz, cristobalite, and coesite; (b) for the disordered structures of tridymite and the clathrasils; and (c) for the substitutionally disordered high albite and sanidine.

All of the refinements for low cristobalite undertaken by Peacor (1973) meet the criteria, with the exception of the one undertaken at 523 K. The failure of this refinement is, however, marginal. All three of the low cristo-

TABLE 2. Silica polymorphs and aluminosilicate frameworks which do not satisfy the rigid-bond criteria of this paper

Mineral	Reference	⟨⟨Δ⟩⟩	Esd
Quartz	Lager et al. (1982), at 13 K	0.00264	0.00118
Quartz	Lager et al. (1982), at 78 K	0.00284	0.00134
Quartz	Lager et al. (1982), at 296 K	0.00749	0.00315
Quartz	Smith and Alexander (1963)	0.00266	0.00070
Quartz	Zachariasen and Plettinger (1965), type I	0.00211	0.00011
Cristobalite	Peacor (1973), at 230 °C	−0.00092	0.00143
Cristobalite	Pluth et al. (1985a), at 10 K	−0.00146	0.00033
Cristobalite	Pluth et al. (1985a), at 293 K	−0.00555	0.00142
Cristobalite	Pluth et al. (1985a), at 473 K	−0.00777	0.00244
Tridymite	Dollase (1967)	0.00331	0.00806
Tridymite	Baur (1977)	0.00077	0.00345
Tridymite	Kihara (1977)	0.00511	0.01996
Tridymite	Kihara (1978)	−0.00136	0.00622
Tridymite	Kihara et al. (1986a), at 443 K	0.01483	0.01160
Tridymite	Kihara et al. (1986a), at 493 K	0.00178	0.01039
Tridymite	Kihara et al. (1986a), at 573 K	0.00502	0.00583
Tridymite	Kihara et al. (1986a), at 653 K	0.00695	0.01199
Tridymite	Kihara et al. (1986a), at 693 K, C222,	0.00032	0.00615
Tridymite	Kihara et al. (1986a), at 693 K, $P6_3/mmc$	−0.00762	0.00554
Tridymite	Kihara et al. (1986a), at 733 K, $P6_3/mmc$	−0.00603	0.00587
Tridymite	Kihara et al. (1986b), at 493 K	−0.00677	0.00466
Tridymite	Kihara et al. (1986b), at 693 K	−0.00486	0.00462
Tridymite	Kihara et al. (1986b), at 733 K	−0.00340	0.00504
Melanophlogite	Gies (1983)	−0.00201	0.00142
Dodecasil *3C*	Gies (1984)	0.00008	0.00509
Dodecasil *1H*	Gerke and Gies (1984)	0.00156	0.01301
Dodecasil *3R*	Gies (1986)	0.02166	0.01285
High albite	Keefer and Brown (1978)	0.00415	0.00331
High albite	Winter et al. (1979), at 25 °C	0.00388	0.00141
High albite	Winter et al. (1979), at 500 °C	0.00500	0.00155
High albite	Winter et al. (1979), at 750 °C	0.00495	0.00163
High albite	Winter et al. (1979), at 980 °C	0.00537	0.00211
Intermediate albite	Phillips et al. (1989)	0.00392	0.00152
Microcline	Blasi et al. (1981)	0.00460	0.00368
Adularia	Phillips and Ribbe (1973)	0.00537	0.00307
Sanidine	Keefer and Brown (1978)	0.00455	0.00151
Sanidine	Phillips and Ribbe (1973)	0.00628	0.00143
Sanidine	Scambos et al. (1987)	0.00553	0.00189
Sanidine	Weitz (1972), Eifel, unheated	0.01245	0.00232
Sanidine	Weitz (1972), Eifel, heated	0.01198	0.00265
Orthoclase	Prince et al. (1973)	0.00221	0.00474
Celsian	Griffen and Ribbe (1976)	0.00472	0.00515
$Cs[AlSi_5O_{12}]$	Araki (1980)	0.00232	0.00229
$RbAlSiO_4$	Klaska and Jarchow (1975)	0.00333	0.00111
Plagioclase	Tagai et al. (1980), An66	0.00327	0.01001
Anorthite	Czank (1973), $P\bar{1}$ at 20 °C	0.00338	0.00298
Anorthite	Czank (1973), $P\bar{1}$ at 240 °C	0.00175	0.00381
Anorthite	Bruno et al. (1976), $I\bar{1}$	0.00222	0.00224
Anorthite	Kalus (1978), $P\bar{1}$	0.00058	0.00204
Anorthite	Wenk and Kroll (1984), An94, $P\bar{1}$	0.00242	0.00141
Anorthite	Angel (pers. comm.), sample 115082a $I\bar{1}$	0.00111	0.00227
Anorthite	Angel (pers. comm.), from Monte Somma, $I\bar{1}$	0.00047	0.00216
Anorthite	Angel (pers. comm.), from Val Pasmeda, $I\bar{1}$	0.00130	0.00365
Anorthite	Angel (pers. comm.), from Val Pasmeda, $P\bar{1}$	0.00018	0.00208
Sr feldspar	Chiari et al. (1975)	0.00205	0.00408
Sr feldspar	Grundy and Ito (1974)	0.00385	0.00279
Low cordierite	Hochella et al. (1979), at 24 °C, Dolni Bory	0.00118	0.00204
Low cordierite	Hochella et al. (1979), at 375 °C, Dolni Bory	0.00009	0.00133
Low cordierite	Hochella et al. (1979), at 775 °C, White Well	0.00038	0.00340
Low cordierite	Wallace and Wenk (1980), sample Brg 50	0.00309	0.00117
Low cordierite	Wallace and Wenk (1980), sample Sci 552	0.00226	0.00071
Low cordierite	Wallace and Wenk (1980), sample Sci 1542	0.00259	0.00060
Low cordierite	Wallace and Wenk (1980), sample Sci 1104	0.00239	0.00094
Leucite	Mazzi et al. (1976), $I4_1/a$	0.00759	0.00350
Leucite	Peacor (1968), *Ia3d*	0.00588	0.00163
Analcime	Pechar (1988)	0.00464	0.00274
Bicchulite	Sahl (1980)	0.00506	—
Brewsterite	Schlenker et al. (1977)	0.00463	0.00215
Brewsterite	Artioli et al. (1985)	0.00458	0.00326
Chabazite	Mortier et al. (1979)	0.00836	0.00183
Clinoptilolite	Koyama and Takéuchi (1977), from Agoura	0.00403	0.00236
Clinoptilolite	Koyama and Takéuchi (1977), from Kuruma	0.00135	0.00350
Edingtonite	Mazzi et al. (1984), Ice River, $P\bar{4}2_1m$	0.00430	0.00056
Edingtonite	Mazzi et al. (1984), Old Kilpatrick, $P\bar{4}2_1m$	0.00412	0.00071
Ferrierite	Vaughan (1966)	0.00962	0.01067
Ferrierite	Gramlich-Meier et al. (1984)	0.00306	0.00779

TABLE 2.—*Continued*

Mineral	Reference	⟨⟨Δ⟩⟩	Esd
Ferrierite	Gramlich-Meier et al. (1985)	0.00563	0.00766
Ferrierite	Alberti and Sabelli (1987)	0.00490	0.00711
Gismondine	Artioli et al. (1986a), at 15 K	0.00065	0.00197
Goosecreekite	Rouse and Peacor (1986)	0.00715	0.00541
Mordenite	Alberti et al. (1986)	0.00409	0.00479
Offretite	Mortier et al. (1976a)	0.00477	0.00538
Offretite	Mortier et al. (1976b)	0.00584	0.00465
Osumilite	Armbruster and Oberhänsli (1988)	0.00504	0.00283
Scolecite	Joswig et al. (1984)	0.00110	0.00194
Stellerite	Galli and Alberti (1975)	0.01894	0.01627
Stellerite	Miller and Taylor (1985)	0.00959	0.00746
Cd-X zeolite	Calligaris et al. (1986), hydrated	0.00458	0.00706
Cd-X zeolite	Calligaris et al. (1986), dehydrated	0.01707	0.01128
Na-X zeolite	Calestani et al. (1987)	0.00938	0.00860
Ca-A zeolite	Thöni (1975)	−0.00204	0.00685
Tl-A zeolite	Thöni (1975)	−0.00175	0.00661

balite refinements completed by Pluth et al. (1985a) fail. The Si atom in these crystals was found to vibrate with a larger amplitude along the SiO bond than the O atom, unlike all the other structures in Table 1. No explanation is offered for this result.

Without exception, all of the coesite structures used to construct Figure 1 satisfy the criteria, as we expect inasmuch as these data were used to establish the criteria. However, an examination of the MSDAs calculated for the SiO bonds of a crystal with $P2_1/a$ space-group symmetry (Kirfel et al., 1979) shows a relatively wide scatter of data (Fig. 7). This scatter of data is consistent with the single crystal X-ray and TEM data reported by Sasaki et al. (1983), which shows that $P2_1/a$ coesite is nothing more than a coesite crystal twinned on {100} (Kirfel and Will, 1984).

All the tridymite and clathrate structures examined in population II fail to meet at least one of the criteria. This includes a twinned low tridymite crystal (Kato and Nukui, 1976) upon which an important conclusion in crystal chemistry has been drawn by Baur (1977) and Baur and Ohta (1982). In a structure analysis of this crystal, Kato and Nukui (1976) were unable to refine simultaneously all of its positional and thermal parameters because of the limited storage capacity of their computer. They also observed that the crystal was twinned about [130]. Despite this crystal defect, Baur (1977) undertook a re-refinement of the structure in which each parameter was allowed to vary. Using the R(SiO) and SiOSi angle data obtained from this refinement together with data obtained for several silica polymorphs, the twinned $P2_1/a$ coesite crystal, and several silicates, Baur and Ohta (1982) completed a linear regression analysis to test whether R(SiO) correlates with $-\sec\angle$(SiOSi). On the basis of the statistics of their results, they concluded that the correlation is not significant, as was also concluded in several earlier studies by Baur (1971, 1977).

The twinned character of the low tridymite crystal used in the Baur and Ohta (1982) analysis is borne out very nicely by the scatter of data displayed in Figure 7. In fact, the relatively wide scatter of points in this plot for both this crystal and for the $P2_1/a$ coesite crystal is consistent with their twinned structures. Inasmuch as 60% of the sample population used in their regression analysis consists of the data used to prepare Figure 7, one is not surprised that Baur and Ohta (1982) found that the correlation is not significant. On the other hand, a stepwise regression analysis of R(SiO) data recorded for a set of silica polymorphs that meet both criteria (Boisen et al., 1990) shows that the correlation between bond length and angle is highly significant, with about 50% of the variation in R(SiO) being explained in terms of a linear dependence upon $-\sec\angle$(SiOSi). Similar correlations have been reported by Taylor (1972), Gibbs et al. (1972), Gibbs et al. (1977a), Gibbs et al. (1977b), Tossell and Gibbs (1977, 1978), Meagher et al. (1979), Hill and Gibbs (1979), Newton and Gibbs (1980), Chakoumakos et al. (1981), Gibbs et al. (1981), O'Keeffe et al. (1985), Gibbs and Boisen (1986), Smyth et al. (1987), and Geisinger et al.

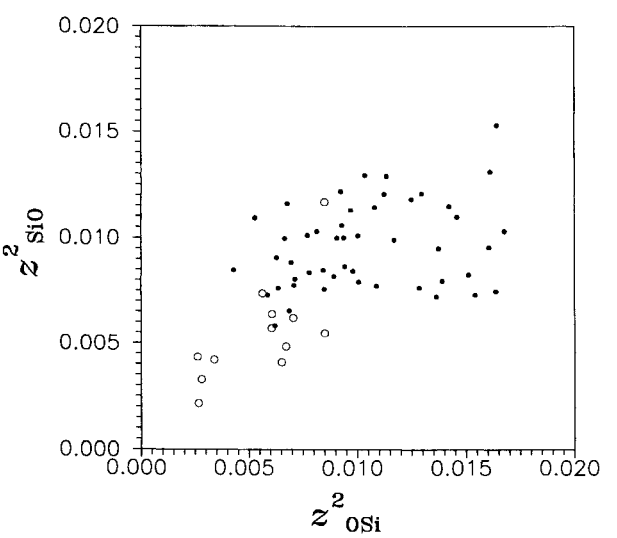

Fig. 7. A scatter diagram of z^2_{SiO} vs. z^2_{OSi} recorded for the tridymite data (solid circles) by Baur (1977) and the $P2_1/a$ coesite data (open circles) recorded by Kirfel et al. (1979).

(1987). Thus, we conclude that the correlation between bond length and angle is genuine, particularly since it has also been reproduced in robust quantum mechanical calculations completed on a variety of hydroxyacid silicate molecules (Newton and Gibbs, 1980; O'Keeffe et al., 1985; Gibbs and Boisen, 1986; Boisen et al., 1990).

All the low albite refinements examined satisfy both criteria. Like the data for coesite, they also were used to establish the criteria, and so this is not an unexpected result. In an examination of the study by Winter et al. (1977) of low albite, a regular increase in $\langle\langle\Delta\rangle\rangle$ and its esd is observed to occur with increasing temperature. As indicated earlier, this supports the suggestion that the TO bonds in this material may weaken somewhat with increasing temperature. The so-called ordered orthoclase crystal refined by Prince et al. (1973) also fails to meet the criteria. A study of its mean TO bond lengths indicates that the T(2) tetrahedra are ordered (Si rich), whereas each T(1) tetrahedra contains a disordered occupancy of one Al and one Si, on average. An examination of the $\langle\Delta\rangle$ values and their esd for these two tetrahedra yields values that agree with these results [T(1)/$\langle\Delta\rangle$ = 0.00466 Å^2, esd = 0.00590 Å^2; T(2)/$\langle\Delta\rangle$ = −0.00023 Å^2, esd = 0.00138 Å^2]. The $\langle\Delta\rangle$ value calculated for the T(1) tetrahedron that contains 0.5 Al and 0.5 Si, on average, agrees with a value of 0.0047 Å^2 calculated, using Equation 2, for a disordered array of Al and Si over the T(1) tetrahedron. The $\langle\Delta\rangle$ value for the T(2) tetrahedron indicates the tetrahedron is ordered and only contains Si, as determined from its mean TO bond lengths.

None of the anorthite crystals that we examined meets the criteria. Angel (personal communication, 1988) refined the Val Pasmeda anorthite in both $I\bar{1}$ and $P\bar{1}$ settings. We find that the $P\bar{1}$ refinement comes the closest to satisfying the criteria, supporting suggestions that the $P\bar{1}$ setting is the more appropriate one for the crystal. Angel's results and those recorded by Czank (1973), Kalus (1978), and Wenk and Kroll (1984) for anorthite suggest that this feldspar may exhibit a small amount of substitutional disorder or twinning despite an Al/Si ratio of 1.0.

Seven of the eighteen structural refinements completed for cordierite and listed in Table 2 fail to meet the criteria. We offer no explanation for these failures.

Of the 34 refinements of zeolites examined, seven [edingtonite (two times), mesolite, natrolite, scolecite, thomsonite, and yugawaralite] satisfy the criteria, whereas the remaining ones fail. All seven of the zeolites that satisfied the criteria are considered to be ordered, within the experimental error, in terms of their mean TO bond lengths. Of the 27 zeolites that failed, 24 are considered to exhibit substitutional disorder. A calculation of the TO bond lengths for one of these zeolites, analcime, using data published by Pechar (1988), yields the following mean TO bond lengths and predicted occupancies: ⟨Si1O⟩ = 1.614, 0.06 Al; ⟨Si2O⟩ = 1.621, 0.11 Al; ⟨Si3O⟩ = 1.621, 0.11 Al; ⟨Si4O⟩ = 1.614, 0.06 Al; ⟨Al1O⟩ = 1.740, 0.89 Al; and ⟨Al2O⟩ = 1.740, 0.89 Al. These results indicate a moderate degree of disorder with a long-range order parameter of s = 0.78. However, a $\langle\langle\Delta\rangle\rangle$ value of 0.0046 Å^2 calculated for this zeolite indicates a disordered structure. This discrepancy is not understood. A $\langle\langle\Delta\rangle\rangle$ value of 0.00065 Å^2 and an esd of 0.00197 Å^2 calculated for the zeolite gismondine suggests a small amount of disorder, in agreement with the Artioli et al. (1986a) statement that the mean TO distances in the zeolite "are consistent with an essentially ordered distribution of Si and Al and the possibility of a minor substitution of excess Si in the Al(1) site." An examination of the mean TO bond lengths in goosecreekite (Rouse and Peacor, 1986) indicates almost complete Si/Al ordering. However, a large $\langle\langle\Delta\rangle\rangle$ value of 0.00715 Å^2 calculated for this zeolite indicates the presence of structural disorder. Mazzi et al. (1984) concluded that tetragonal edingtonite is completely disordered. The $\langle\langle\Delta\rangle\rangle$ and the esd calculated for these zeolites conform with this result. The Cd-X zeolite refined by Calligaris et al. (1986) shows, after dehydration, a substantial increase in Δ values, with the $\langle\langle\Delta\rangle\rangle$ values increasing from 0.00458 Å^2 to 0.01707 Å^2. This suggests that dehydration may induce some form of disorder where the unit cells in the structure collapse in different orientations, disrupting the translational symmetry of the crystal.

Finally, the MSDAs of the T and O atoms of framework structures provide criteria by which the perfection of a crystal may be judged. As static disorder can have a pernicious effect on the observed bond lengths and angles obtained in a diffraction experiment, it is important that future crystal chemical studies be undertaken with data selected for crystals that satisfy criteria of the type set forth in this paper. Otherwise, meaningful correlations could be rejected as statistically insignificant because of systematic errors.

The consequences of a rigid bond model on the orientation of the displacement ellipsoid of a bridging O atom

In an earlier study of the displacement ellipsoids recorded for othopyroxene, Burnham et al. (1971) observed that the major axis of the ellipsoid for each bridging O atom is perpendicular to the SiOSi plane. Also, Schulz (1972) observed that the major axes of the displacement ellipsoids of the O atoms in framework aluminosilicates tend to be perpendicular to the TOT plane, that their minor axes tend to parallel the TT direction, and that their intermediate axes tend to lie in the TOT plane perpendicular to the TT direction. In the appendix of this paper, we will examine the extent to which these observations can be explained in terms of a simple rigid bond model and the extent to which this orientation is governed by the size of the TOT angle.

Each O atom in a framework structure is shared between two T atoms in forming two TO bonds defining a TOT group. A model in which these bonds are assumed to be rigid can be used to predict the orientation and shape of the displacement ellipsoid of the bridging O rel-

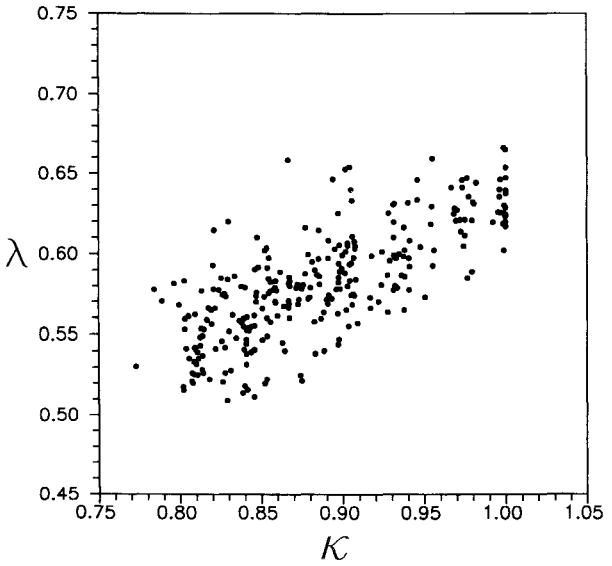

Fig. 8. A scatter plot of observed ellipticity, λ, of the ellipse defined by the short and intermediate axis of the displacement ellipsoid of O vs. the ellipticity, κ, calculated from a rigid bond model.

ative to the TOT group. Using the bisector *l* of the TOT angle as a frame of reference, we will see that the model predicts, for TOT angles typically observed for silicates, that the shortest axis of the ellipsoid should tend to lie in the TOT plane perpendicular to *l*, the intermediate axis should lie along *l*, and the longest axis should be perpendicular to the TOT plane, as is consistent with the observation of Schulz (1972). Furthermore, the model indicates that the extent to which the shortest axis should tend to the indicated direction depends on the size of the TOT angle with the tendency increasing with a widening of the TOT angle. This prediction is borne out by the analysis presented in the Appendix of the orientations of the observed displacement ellipsoids. The model also predicts a shape for the ellipse, in the plane of the short and intermediate axes, as a function of the TOT angle. In Figure 8 we compare this prediction with the observed orientations and find that the model explains 57% of the variation in the ellipticity of these ellipses (see Appendix 1).

In conclusion, the tetrahedral groups in framework structures behave as if they were rigid bodies. Therefore, in a structural analysis of a well-ordered framework structure one would expect to find that the MSDAs of the T and O atoms along the TO bonds to be equal and that the thermal ellipsoid of the O atom be narrow in the direction of the bond and elongated in the direction perpendicular to the TOT plane. When these conditions are not satisfied, one should consider the possibility of static disorder.

Acknowledgments

We thank the National Science Foundation for its generous support of this study with grant EAR-8803933. We also thank James Burgmeier for allowing us to use the program Epic (written by James Burgmeier and Larry Kost) and Larry W. Finger for his encouraging review.

References cited

Alberti, A., and Sabelli, C. (1987) Statistical and true symmetry of ferrierite: Possible absence of straight T-O-T bridging bonds. Zeitschrift für Kristallographie, 178, 249–256.

Alberti, A., Davoli, P., and Vezzalini, G. (1986) The crystal structure refinement of a natural mordenite. Zeitschrift für Kristallographie, 175, 249–256.

Araki, T. (1980) Crystal structure of a cesium aluminosilicate, $Cs[AlSi_5O_{12}]$. Zeitschrift für Kristallographie, 152, 207–213.

Armbruster, T. (1986a) Role of Na in the structure of low-cordierite: A single-crystal X-ray study. American Mineralogist, 71, 746–757.

——— (1986b) Crystal structure refinement and thermal expansion of a Li, Na, Be-cordierite between 100 and 550 K. Zeitschrift für Kristallographie, 174, 205–217.

Armbruster, T., and Oberhänsli, R. (1988) Crystal chemistry of double-ring silicates: Structural, chemical and optical variations in osumilites. American Mineralogist, 73, 585–594.

Armbruster, T., Bürgi, H.B., Kunz, M., Gnos, E., Brönnimann, S., and Lienert, C. (1990) Variation of displacement parameters in structure refinements of low albite. American Mineralogist, 75, 135–140.

Artioli, G., Smith, J.V., and Kvick, Å. (1984) Neutron diffraction study of Natrolite, $Na_2Al_2Si_3O_{10}\cdot 2H_2O$, at 20 K. Acta Crystallographica, C40, 1658–1662.

——— (1985) Multiple hydrogen positions in the zeolite brewsterite $(Sr_{.93},Ba_{.05})Al_2Si_6O_{16}\cdot 5H_2O$. Acta Crystallographica, C41, 492–497.

Artioli, G., Rinaldi, R., Kvick, Å., and Smith, J.V. (1986a) Neutron diffraction structure refinement of the zeolite gismondine at 15 K. Zeolites, 6, 361–366.

Artioli, G., Smith, J.V., and Pluth, J.J. (1986b) X-ray structure refinement of mesolite. Acta Crystallographica, C42, 937–942.

Baur, W.H. (1971) The prediction of bond length variations in silicon-oxygen bonds. American Mineralogist, 56, 1573–1599.

——— (1977) Silicon-oxygen bond lengths, bridging angles Si-O-Si and synthetic low tridymite. Acta Crystallographica, B33, 2615–2619.

Baur, W.H., and Ohta, T. (1982) The Si_5O_{16} pentamer in zunyite refined and empirical relations for individual silicon-oxygen bonds. Acta Crystallographica, B38, 390–401.

Bissert, G., and Liebau, F. (1986) The crystal structure of a triclinic bikitaite, $Li[AlSi_2O_6]\cdot H_2O$, with ordered Al/Si distribution. Neues Jahrbuch für Mineralogie Monatshefte, 1986, 241–252.

Blasi, A., De Pol Blasi, C., and Zanazzi, P.F. (1981) Structural study of a complex microperthite from anatexites at Mt. Caval, Argentera Massif, Maritime Alps. Neues Jahrbuch für Mineralogie Abhandlungen, 142, 71–90.

Blasi, A., Brajkovic, A., De Pol Blasi, C., Foord, E.E., Martin, R.F., and Zanazzi, P.F. (1984) Structure refinement and genetic aspects of a microcline over-growth on amazonite from Pikes Peak batholith, Colorado, U.S.A. Bulletin de Minéralogie, 107, 411--422.

Blasi, A., De Pol Blasi, C., and Zanazzi, P.F. (1987) A re-examination of the Pellotsalo microcline: Mineralogical implications and genetic considerations. Canadian Mineralogist, 25, 527–537.

Boisen, M.B., Jr., Gibbs, G.V., Downs, R.T., and D'Arco, P. (1990) The dependence of the SiO bond length on structural parameters in coesite, the silica polymorphs and the clathrasils. American Mineralogist, 75, 748–754.

Bruno, E., Chiari, G., and Facchinelli, A. (1976) Anorthite quenched from 1530 °C. I. Structural refinement. Acta Crystallographica, B32, 3270–3280.

Bürgi, H.B. (1984) Stereochemical lability in crystalline coordination compounds. Transactions of the American Crystallographic Association, 20, 61–71.

——— (1989) Interpretation of atomic displacement parameters: Intramolecular translational oscillation and rigid-body motion. Acta Crystallographica, B45, 383–390.

Burnham, C.W., Ohashi, Y., Hafner, S.S., and Virgo, D. (1971) Cation distribution and atomic thermal vibrations in a iron-rich orthopyroxene. American Mineralogist, 56, 850–876.

Calestani, G., Bacca, G., and Andreetti, G.D. (1987) Structural study of zeolite X exchanged with 'f' transition elements. I. Crystal structure of reference hydrated Na-X. Zeolites, 7, 54–58.

Calligaris, M., Nardin, G., Randaccio, L., and Zangrando, E. (1986) Crystal structures of the hydrated and partially dehydrated forms of Cd-X exchanged zeolites. Zeolites, 6, 439–444.

Chakoumakos, B.C., Hill, R.J., and Gibbs, G.V. (1981) A molecular orbital study of rings in silicates and siloxanes. American Mineralogist, 66, 1237–1249.

Chiari, G., Calleri, M., Bruno, E., and Ribbe, P.H. (1975) The structure of partially disordered synthetic strontium feldspar. American Mineralogist, 60, 111–119.

Cohen, J.P., Ross, F.K., and Gibbs, G.V. (1977) An X-ray and neutron diffraction study of hydrous low cordierite. American Mineralogist, 62, 67–78.

Czank, M. (1973) Strukturuntersuchungen von Anorthit in Temperaturbereich von 20 °C bis 1430 °C. Dissertation, Eidgenössische Technische Hochschule, Zurich.

Dollase, W.A. (1967) The crystal structure at 220 °C of orthorhombic high tridymite from the Steinbach Meteorite. Acta Crystallographica, 23, 617–623.

Downs, R.T. (1989) A study of the mean-square displacement amplitudes of T and O atoms in framework silicates and aluminosilicates: Evidence for rigid TO bonds, disorder, twinning, and stacking faults in crystals. M.S. thesis, Virginia Polytechnic Institute and State University, Blacksburg, Virginia.

Dunitz, J.D., Schomaker, V., and Trueblood, K.N. (1988) Interpretation of atomic displacement parameters from diffraction studies of crystals. The Journal of Physical Chemistry, 92, 856–867.

Flörke, O.W. (1954) Die Ursachen der Hoch-Tief-Umwandlungsanomalie von Tridymit und Cristobalit. Naturwissenschaften, 41, 371–372.

——— (1955) Strukturanomalien bei Tridymit und Cristobalit. Beriche der Deutschen Keramischen Gesellschaft, 32, 369–381.

Frondel, C. (1962) The System of Mineralogy, vol. 3, Silica Minerals. Wiley, New York.

Galli, E. (1976) Crystal structure refinement of edingtonite. Acta Crystallographica, B32, 1623–1627.

Galli, E., and Alberti, A. (1975) The crystal structure of stellerite. Bulletin de la Société française de Minéralogie et de Cristallographie, 98, 11–18.

Geisinger, K.L., Gibbs, G.V., and Navrotsky, A. (1985) A molecular orbital study of bond length and angle variations in framework structures. Physics and Chemistry of Minerals, 11, 266–283.

Geisinger, K.L., Spackman, M.A., and Gibbs, G.V. (1987) Exploration of structure, electron density distribution and bonding in coesite with Fourier and pseudoatom refinement methods using single-crystal X-ray diffraction data. The Journal of Physical Chemistry, 91, 3237–3244.

Gerke, H., and Gies, H. (1984) Studies on clathrasils. IV: Crystal structure of dodecasil 1H, a synthetic clathrate compound of silica. Zeitschrift für Kristallographie, 166, 11–22.

Ghose, S., Schomaker, V., and McMullan, R.K. (1986) Enstatite, $Mg_2Si_2O_6$: A neutron diffraction refinement of the crystal structure and a rigid-body analysis of the thermal vibration. Zeitschrift für Kristallographie, 176, 159–175.

Gibbs, G.V., and Boisen, M.B., Jr. (1986) Molecular mimicry of structure and electron density distributions in minerals. Materials Research Society Symposium Proceedings, Better Ceramics through Chemistry, 73, 515–527.

Gibbs, G.V., Hamil, M.M., Louisnathan, S.J., Bartell, L.S., and Yow, H. (1972) Correlations between Si-O bond length, Si-O-Si angle and bond overlap populations calculated using extended Hückel molecular orbital theory. American Mineralogist, 57, 1578–1613.

Gibbs, G.V., Meagher, E.P., Smith, J.V., and Pluth, J.J. (1977a) Molecular orbital calculations for atoms in the tetrahedral frameworks of zeolites. ACA Symposium Series, no. 40, Molecular Sieves—IV, James R. Katzer, Ed., 19–28.

Gibbs, G.V., Prewitt, C.T., and Baldwin, K.J. (1977b) A study of the structural chemistry of coesite. Zeitschrift für Kristallographie, 145, 108–123.

Gibbs, G.V., Meagher, E.P., Newton, M.D., and Swanson, D.K. (1981) A comparison of experimental and theoretical bond length and angle variations for minerals, inorganic solids, and molecules. In M. O'Keeffe and A. Navrotsky, Eds., Structure and bonding in crystals, vol. 1, p. 195–225, Academic Press, New York.

Gies, H. (1983) Studies on clathrasils. III. Crystal structure of melanophlogite, a natural clathrate compound of silica. Zeitschrift für Kristallographie, 164, 247–257.

——— (1984) Studies on clathrasils. VI. Crystal structure of dodecasil 3C, another synthetic clathrate compound of silica. Zeitschrift für Kristallographie, 167, 73–82.

——— (1986) Studies on clathrasils. IX. Crystal structure of deca-dodecasil 3R, the missing link between zeolites and clathrasils. Zeitschrift für Kristallographie, 175, 93–104.

Gramlich-Meier, R., Meier, W.M., and Smith, B.K. (1984) On faults in the framework structure of the zeolite ferrierite. Zeitschrift für Kristallographie, 169, 201–210.

Gramlich-Meier, R., Gramlich, V., and Meier, W.M. (1985) The crystal structure of the monoclinic variety of ferrierite. American Mineralogist, 70, 619–623.

Griffen, D.T., and Ribbe, P.H. (1976) Refinement of the crystal structure of celsian. American Mineralogist, 61, 414–418.

Griffen, D.T., Ribbe, P.H., and Gibbs, G.V. (1977) The structure of slawsonite, a strontium analog of paracelsian. American Mineralogist, 62, 31–35.

Grundy, H.D., and Ito, J. (1974) The refinement of the crystal structure of a synthetic non-stoichiometric Sr feldspar. American Mineralogist, 59, 1319–1326.

Harlow, G.E., and Brown, G.E., Jr. (1980) Low albite: An X-ray and neutron diffraction study. American Mineralogist, 65, 986–995.

Hill, R.J., and Gibbs, G.V. (1979) Variation in d(T − O), d(T . . . T) and ∠TOT in silica and silicate minerals, phosphates and aluminates. Acta Crystallographica, B35, 25–30.

Hirshfeld, F.L. (1976) Can X-ray data distinguish bonding effects from vibrational smearing. Acta Crystallographica, A32, 239–244.

Hochella, M.F., Jr., Brown, G.E., Jr., Ross, F.K., and Gibbs, G.V. (1979) High-temperature crystal chemistry of hydrous Mg- and Fe-cordierites. American Mineralogist, 64, 337–351.

Joswig, W., Bartl, H., and Fuess, H. (1984) Structure refinement of scolecite by neutron diffraction. Zeitschrift für Kristallographie, 166, 219–223.

Kalus, C. (1978) Neue Strukturbestimmung des Anorthits unter Berücksichtigung möglicher Alternativen. Dissertation, Ludwig-Maximilians-Universität, Munich.

Kato, K., and Nukui, A. (1976) Die Kristallstruktur des monoklinen Tief-Tridymits. Acta Crystallographica, B32, 2486–2491.

Keefer, K.D., and Brown, G.E., Jr. (1978) Crystal structures and compositions of sanidine and high albite in cryptoperthitic intergrowth. American Mineralogist, 63, 1264–1273.

Kihara, K. (1977) An orthorhombic superstructure of tridymite existing between about 105 and 180 °C. Zeitschrift für Kristallographie, 146, 185–203.

——— (1978) Thermal change in unit-cell dimensions and a hexagonal structure of tridymite. Zeitschrift für Kristallographie, 148, 237–253.

Kihara, K., Matsumato, T., and Imamura, M. (1986a) Structural change of orthorhombic-I tridymite with temperature: A study based on second-order thermal vibrational parameters. Zeitschrift für Kristallographie, 177, 27–38.

——— (1986b) High-order thermal-motion tensor analyses of tridymite. Zeitschrift für Kristallographie, 177, 39–52.

Kirfel, A., and Will, G. (1984) Ending the "$P2_1/a$ coesite" discussion. Zeitschrift für Kristallographie, 167, 287–291.

Kirfel, A., Will, G., and Arndt, J. (1979) A new phase of coesite SiO_2. Zeitschrift für Kristallographie, 149, 315–326.

Klaska, R., and Jarchow, O. (1975) Die Kristallstruktur und die Verzwillingung von $RbAlSiO_4$. Zeitschrift für Kristallographie, 142, 225–238.

Koyama, K., and Takéuchi, Y. (1977) Clinoptilolite: The distribution of potassium atoms and its role in thermal stability. Zeitschrift für Kristallographie, 145, 216–239.

Kunz, M., and Armbruster, T. (1990) Difference displacement parameters

in alkali feldspars: Effect of (Si,Al) order-disorder. American Mineralogist, 75, 141–149.
Kvick, Å., and Smith, J.V. (1983) A neutron diffraction study of the zeolite edingtonite. The Journal of Chemical Physics, 79, 2356–2362.
Kvick, Å., Ståhl, K., and Smith, J.V. (1985) A neutron diffraction study of the bonding of zeolitic water in scolecite at 20 K. Zeitschrift für Kristallographie, 171, 141–154.
Kvick, Å., Artioli, G., and Smith, J.V. (1986) Neutron diffraction study of the zeolite yugawaralite at 13 K. Zeitschrift für Kristallographie, 174, 265–281.
Lager, G.A., Jorgensen, J.D., and Rotella, F.J. (1982) Crystal structure and thermal expansion of α-quartz SiO_2 at low temperatures. The Journal of Applied Physics, 53, 6751–6756.
Le Page, Y., and Donnay, G. (1976) Refinement of the crystal structure of low-quartz. Acta Crystallographica, B32, 2456–2459.
Levien, L., and Prewitt, C.T. (1981) High-pressure crystal structure and compressibility of coesite. American Mineralogist, 66, 324–333.
Levien, L., Prewitt, C.T., and Weidner, D.J. (1980) Structure and elastic properties of quartz at pressure. American Mineralogist, 65, 920–930.
Liebau, F. (1985) Structural chemistry of silicates: Structure, bonding and classification. Springer-Verlag, Berlin.
Mazzi, F., Galli, E., and Gottardi, G. (1976) The crystal structure of tetragonal leucite. American Mineralogist, 61, 108–115.
——— (1984) Crystal structure refinement of two tetragonal edingtonites. Neues Jahrbuch für Mineralogie Monatshefte, 1984, 373–382.
Meagher, E.P., Tossell, J.A., and Gibbs, G.V. (1979) A CNDO/2 molecular orbital study of the silica polymorphs quartz, cristobalite and coesite. Physics and Chemistry of Minerals, 4, 11–21.
Megaw, H.D. (1973) Crystal structures: A working approach. W.B. Saunders Co., Philadelphia, Pennsylvania, 399–434.
——— (1974) The architecture of the feldspars. In W.S. MacKenzie and J. Zussman, Eds., The feldspars, Manchester University Press, Manchester, England.
Miller, S.A., and Taylor, J.C. (1985) Neutron single crystal diffraction study of an Australian stellerite. Zeolites, 5, 7–10.
Mortier, W.J., Pluth, J.J., and Smith, J.V. (1976a) The crystal structure of dehydrated natural offretite with stacking faults of erionite type. Zeitschrift für Kristallographie, 143, 319–332.
——— (1976b) Crystal structure of natural zeolite offretite after carbon monoxide adsorption. Zeitschrift für Kristallographie, 144, 32–41.
Mortier, W.J., King, G.S.D., and Sengier, L. (1979) Crystal structures of dehydrated II chabazite pretreated at 320 °C and at 600 °C after steaming. Journal of Physical Chemistry, 83, 2263–2266.
Newton, M.D., and Gibbs, G.V. (1980) *Ab initio* calculated geometries and charge distributions for H_4SiO_4 and $H_6Si_2O_7$ compared with experimental values for silicates and siloxanes. Physics and Chemistry of Minerals, 6, 221–246.
O'Keeffe, M., Domengès, B., and Gibbs, G.V. (1985) *Ab initio* molecular orbital calculation on phosphates: Comparison with silicates. The Journal of Physical Chemistry, 89, 2304–2309.
Peacor, D.R. (1968) A high temperature single crystal diffractometer study of leucite, $(K,Na)AlSi_2O_6$. Zeitschrift für Kristallographie, 127, 213–224.
——— (1973) High-temperature single-crystal study of the cristobalite inversion. Zeitschrift für Kristallographie, 138, 274–298.
Pechar, F. (1988) The crystal structure of natural monoclinic analcime ($NaAlSi_2O_6 \cdot H_2O$). Zeitschrift für Kristallographie, 184, 63–69.
Phillips, M.W., and Ribbe, P.H. (1973) The structures of monoclinic potassium-rich feldspars. American Mineralogist, 58, 263–270.
Phillips, M.W., Ribbe, P.H., and Pinkerton, A.A. (1989) The structure of intermediate albite, $NaAlSi_3O_8$. Acta Crystallographica, C45, 542–545.
Pluth, J.J., Smith, J.V., and Faber, J., Jr. (1985a) Crystal structure of low cristobalite at 10, 293 and 473 K: Variation of framework geometry with temperature. The Journal of Applied Physics, 57, 1045–1049.
Pluth, J.J., Smith, J.V., and Kvick, Å. (1985b) Neutron diffraction study of the zeolite thomsonite. Zeolites, 5, 74–80.
Prince, E., Donnay, G., and Martin, R.F. (1973) Neutron diffraction refinement of an ordered orthoclase structure. American Mineralogist, 58, 500–507.
Rouse, R.C., and Peacor, D.R. (1986) Crystal structure of the zeolite mineral goosecreekite, $CaAl_2Si_6O_{16} \cdot 5H_2O$. American Mineralogist, 71, 1494–1501.
Sahl, K. (1980) Refinement of the crystal structure of bicchulite, $Ca_2[Al_2SiO_6](OH)_2$. Zeitschrift für Kristallographie, 152, 13–21.
Sasaki, S., Chen, H-K., Prewitt, C.T., and Nakajima, Y. (1983) Re-examination of "$P2_1/a$ coesite." Zeitschrift für Kristallographie, 164, 67–77.
Scambos, T.A., Smyth, J.R., and McCormick, T.C. (1987) Crystal-structure refinement of high sanidine from the upper mantle. American Mineralogist, 72, 973–978.
Schlenker, J.L., Pluth, J.J., and Smith, J.V. (1977) Refinement of the crystal structure of brewsterite, $Ba_{0.5}Sr_{1.5}Al_4Si_{12}O_{32} \cdot 10H_2O$. Acta Crystallographica, B33, 2907–2910.
Schulz, H. (1972) Influence of "split" atoms on anisotropic temperature factors (shown at the example of quartz-like silicates of composition $Li_2O \cdot Al_2O_3 \cdot xSiO_2$ with $x \geq 2$). Zeitschrift für Kristallographie, 136, 321–349.
Smith, G.S., and Alexander, L.E. (1963) Refinement of the atomic parameters of α-quartz. Acta Crystallographica, 16, 462–471.
Smith, J.V. (1954) A review of the Al-O and Si-O distances. Acta Crystallographica, 7, 479–481.
Smith, J.V., and Bailey, S.W. (1963) Second review of Al-O and Si-O tetrahedral distances. Acta Crystallographica, 16, 801–811.
Smith, J.V., Artioli, G., and Kvick, Å. (1986) Low albite, $NaAlSi_3O_8$: Neutron diffraction study of crystal structure at 13 K. American Mineralogist, 71, 727–733.
Smyth, J.R., Smith, J.V., Artioli, G., and Kvick, Å. (1987) Crystal structure of coesite, a high-pressure form of SiO_2, at 15 and 298 K from single-crystal neutron and X-ray diffraction data: Test of bonding models. The Journal of Physical Chemistry, 91, 988–992.
Strob, W.D. (1981) Strukturverfeinerung eines Tief-Mikroklins, Zusammenhänge zwischen ⟨T − O⟩ Abständen und Al, Si-Ordnungsgrad und metrische Variation in einer Tief-Albit/Tief-Mikroklin–Mischkristallreihe. Dissertation, Westfälische Wilhelms-Universität, Münster, Germany.
Tagai, T., Joswig, W., and Korekawa, M. (1980) Die Bestimmung der Al/Si-Verteilung mittels Neutronenbeugung in einem Plagioklas An_{66}. Zeitschrift für Kristallographie, 151, 77–89.
Taylor, D. (1972) The relationship between Si-O distances and Si-O-Si bond angle in the silica polymorphs. The Mineralogical Magazine, 38, 629–631.
Thöni, W. (1975) The crystal structure of hydrated zeolites T1-A, Ca-A and Ag-A. Zeitschrift für Kristallographie, 142, 142–160.
Tossell, J.A., and Gibbs, G.V. (1977) Molecular orbital studies of geometries and spectra of minerals and inorganic compounds. Physics and Chemistry of Minerals, 2, 21–57.
——— (1978) The use of molecular-orbital calculations on model systems for prediction of bridging-bond-angle variations in siloxanes, silicates, silicon nitrides and silicon sulfides. Acta Crystallographica, A34, 463–472.
Tsuneyuki, S., Aoki, H., Tsukada, M., and Matsui, Y. (1990) Molecular-dynamics study of the α to β structural phase transition of quartz. Physical Review Letters, 64, 776–779.
Vaughan, P.A. (1966) The crystal structure of the zeolite ferrierite. Acta Crystallographica, 21, 983–990.
Wallace, J.H., and Wenk, H.R. (1980) Structural variation in low cordierites. American Mineralogist, 65, 96–111.
Weitz, G. (1972) Die Struktur des Sanidins bei verschiedenen Ordnungsgraden. Zeitschrift für Kristallographie, 136, 418–426.
Wenk, H.R., and Kroll, H. (1984) Analysis of $P\bar{1}$, $I\bar{1}$ and $C\bar{1}$ plagioclase structures. Bulletin de Minéralogie, 107, 467–487.
Willis, B.T.M., and Pryor, A.W. (1975) Thermal vibrations in crystallography. Cambridge University Press, Cambridge, England.
Winter, J.K., Ghose, S., and Okamura, F.P. (1977) A high-temperature study of the thermal expansion and the anisotropy of the sodium atom in low albite. American Mineralogist, 62, 921–931.
Winter, J.K., Okamura, F.P., and Ghose, S. (1979) A high-temperature structural study of the high albite, monalbite and the analbite → monalbite phase transition. American Mineralogist, 64, 409–423.
Wright, A.F., and Lehmann, M.S. (1981) The structure of quartz at 25

and 590 °C determined by neutron diffraction. The Journal of Solid State Chemistry, 36, 371–380.
Young, R.A., and Post, B. (1962) Electron density and thermal effects in alpha quartz. Acta Crystallographica, 15, 337–346.
Zachariasen, W.H. (1969) Concluding remarks. Acta Crystallographica, A25, 276.
Zachariasen, W.H., and Plettinger, H.A. (1965) Extinction in quartz. Acta Crystallographica, 18, 710–714.

Manuscript received March 5, 1990
Manuscript accepted October 10, 1990

Appendix 1. A simple rigid bond model

The basic assumption underlying the rigid bond model is that the stretching of the TO bonds should be minimal. As a measure of the stretching, S, of these bonds due to the motion of the O atom, we use the following formulation:

$$S = (R_1 - R_1')^2 + (R_2 - R_2')^2 \quad (3)$$

where R_1' and R_2' are the observed TO bond lengths defining the TOT group drawn in Appendix Figure 1. In this model, we assume that the O atom is displaced from its observed position by the vector **v** with the constraint, made by Bürgi (1989), that the positions of the T atoms are fixed, resulting in the stretched bond lengths R_1' and R_2'. We define v to be the length of **v**, γ to be the angle between **v** and its projection, **p**, onto the TOT plane, ϕ to be the angle between l and **p**, and Θ to be the TOT angle as shown in the figure. Defining the angles between **p** and R_1 and **p** and R_2 to be $\Psi_1 = \phi + \Theta/2$ and $\Psi_2 = \phi - \Theta/2$, respectively, Equation 3 becomes

$$S = (R_1 - \sqrt{v^2 + R_1^2 - 2vR_1 \cos\gamma \cos\Psi_1})^2 + (R_2 - \sqrt{v^2 + R_2^2 - 2vR_2 \cos\gamma \cos\Psi_2})^2$$

A measure of the resistance to an increase in S, in a given direction defined by ϕ and γ, is the second derivative, K, of S with respect to v at $v = 0$. Evaluating this second derivative, we find that

$$K(\Theta, \gamma, \phi) = 2\cos^2\gamma\left[\cos^2\left(\phi + \frac{\Theta}{2}\right) + \cos^2\left(\phi - \frac{\Theta}{2}\right)\right]$$
$$= 2\cos^2\gamma(1 + \cos\Theta\cos 2\phi). \quad (4)$$

To find the directions in which this resistance has its extreme values, we take the partial derivatives of K with respect to γ and ϕ and set them equal to zero. Doing this, we find the extrema to be in the directions of $\gamma = 90°$ with any ϕ value and $\gamma = 0°$ with ϕ equal to either 0° or 90°. Since the observed Θ values in framework silicates are always greater than 90° (Geisinger et al., 1985), the maximum resistance is in the direction $\gamma = 0°$ and $\phi = 90°$, the intermediate resistance is in the direction $\gamma = \phi = 0°$, and the least resistance is in the direction of $\gamma = 90°$. Hence the expected optimum orientation should be such that the direction of least displacement of the bridging O is in the TOT plane perpendicular to l (roughly parallel to the TT direction). The intermediate displacement should be along l, and the greatest displacement should be perpendicular to the TOT plane. Note that when $\Theta = 180°$, the intermediate and least resistances are predicted to be equal, and so in this case the displacement ellipsoid is predicted to have a circular section perpendicular to the TT direction.

We now consider the question of the variations in the magnitudes of the principal axes of the displacement ellipsoid. When $\gamma = 90°$, the value of K is zero, and so there is no variation in the value of K in the direction of the longest axis. The magnitudes of the other two axes vary with the value of Θ. The model suggests that there should be a relationship between the relative magnitudes of these axes and the relative sizes of the corresponding values of K. Hence we compare the parameters λ and κ defined by

$$\lambda = \frac{L_1}{L_1 + L_S}$$

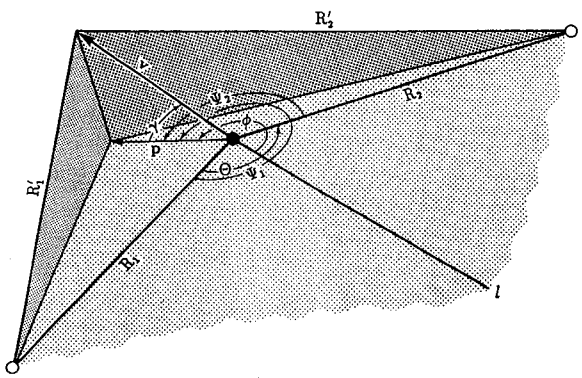

Appendix Fig. 1. A drawing of a TOT group where the T atoms are denoted by open circles and the O atom is denoted by a closed circle. The lengths of the TO bonds are denoted R_1 and R_2, Θ denotes the TOT angle, and l is the bisector of Θ. A displacement, **v**, of the O atom from its equilibrium position, assuming that the T atoms are fixed in space, results in new TO bond lengths, R_1' and R_2'. The vector **p** is the projection of **v** onto the TOT plane, and γ is defined to be the angle between **p** and **v**. The angle between R_1 and **p** is denoted Ψ_1, that between R_2 and **p** is denoted Ψ_2, and that between l and **p** is denoted ϕ.

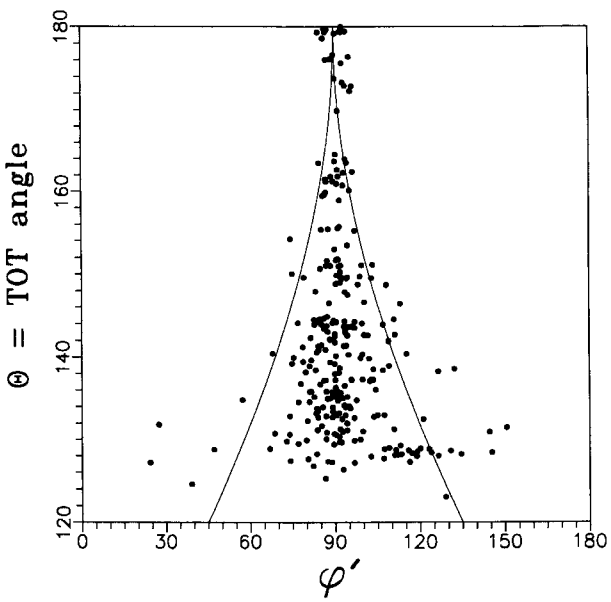

Appendix Fig. 2. A scatter plot of the ϕ' angle of the short axis of the displacement ellipsoid of O vs. the TOT angle, Θ, for the data of Figures 1 and 3. The separation of the curves for a given value of Θ equals $R(\Theta) = 90[2 - A(\Theta)]$.

and

$$\kappa = \frac{K(\Theta, 0, 90)}{K(\Theta, 0, 90) + K(\Theta, 0, 0)}$$

where L_I and L_S are the observed magnitudes of the intermediate and shortest axes of the displacement ellipsoid, respectively. A scatter diagram of λ vs. κ for all of the data used to prepare Figures 1 and 3 is shown in Figure 8. A regression analysis of this data shows that the slope (0.45) is significantly different from zero and that the intercept is 0.18.

Restricting our attention to the TOT plane, we can explain, using Equation 4 with $\gamma = 0°$, the degree to which the short axis of the displacement ellipsoid should prefer the $\phi = 90°$ direction as a function of Θ. For a fixed value of Θ, K is a periodic function of ϕ with an amplitude, $A(\Theta) = 2\|\cos(\Theta)\|$. Since $A(\Theta)$ is the difference between the maximum and minimum resistance, it measures the degree to which the optimum orientation should be preferred. Since A(90) = 0, the model predicts, when $\Theta = 90°$, that there is no preferred orientation of the short axis in the TOT plane, and so it can adopt all ϕ values from $-90°$ to $90°$ (a range of 180°). When $\Theta = 180°$, $A(180)$ equals its maximum value of 2, and so the short axis is predicted to strongly tend to a ϕ value of 90° (a range of 0°). We will define a function R(Θ) that is designed to describe the range of dispersion of the ϕ angles of the short axis. As observed above, we want $R(180) = 0$ and $R(90) = 180$. Therefore, we define $R(\Theta) = 90[2 - A(\theta)]$, which is linearly related to $A(\Theta)$ and passes through the desired points. Appendix Figure 2 shows a scatter diagram of the ϕ'-values observed for the short axis versus Θ values for the data used to construct Figures 1 and 3. We define ϕ' to be the angle between l and the observed short axis. When the short axis is actually found to lie in the TOT plane, then $\phi' = \phi$. These data fall, by and large, between the branches of the drawn curve (Appendix Figure 2) which were placed symmetrically about the line $\phi' = 90°$ such that the width between the branches at a given Θ-value is R(Θ). Thus, as the TOT angle approaches 180°, the ϕ' angle of the short axis of the displacement ellipsoid of the O atom is progressively constrained to adopt an angle of 90° as observed in Appendix Figure 2.